Key Points:

- The negative drought impacts on the upper Yangtze River basin vegetation are more pronounced in late seasons than in other stages
- The faster response of grasslands mainly contributes to the negative impact of late-season droughts
- The complex terrain of basins across the globe results in varying seasonal response patterns to drought

Temporal and Phenological Modulation of the Impact of Increasing Drought Conditions on Vegetation Growth in a Humid Big River Basin: Insights From Global Comparisons

Junlan Xiao[1,2,3] , César Terrer[4] , Pierre Gentine[5] , Ryunosuke Tateno[6] , Lei Fan[1] , Mingguo Ma[1] , Yuemin Yue[7] , Wenping Yuan[8] , Josep Peñuelas[2,3] , and Weiyu Shi[1]

[1]Chongqing Jinfo Mountain Karst Ecosystem National Observation and Research Station, School of Geographical Sciences, Southwest University, Chongqing, China, [2]CSIC, Global Ecology Unit CREAF-CSIC-UAB, Bellaterra, Spain, [3]CREAF, Catalonia, Spain, [4]Department of Civil and Environmental Engineering, Massachusetts Institute of Technology, Cambridge, MA, USA, [5]Department of Earth and Environmental Engineering, Columbia University, New York, NY, USA, [6]Filed Science Education and Research Center, Kyoto University, Kyoto, Japan, [7]Huanjiang Observation and Research Station for Karst Ecosystem, Chinese Academy of Sciences, Huanjiang, China, [8]Institute for Earth System Science, College of Urban and Environmental Sciences, Peking University, Beijing, China

Abstract As the upward trend in extreme drought continues with climate change, terrestrial vegetation growth is assumed to become largely reduced. We investigated anomalies of remote sensing vegetation indexes under droughts across the upper Yangtze River (UYR) basin, characterized as humid but having experienced frequent seasonal droughts from 2000. Then we compared global big river basins by focusing on the Nile and Congo basins, which have similar characteristics to the UYR. The vegetation across the UYR was affected by water stress in recent years but shows reduced sensitivity to drought. The compound effect of drought timing and phenology largely drives the response. Results show that late-season droughts generally have a greater impact on vegetation growth compared to early season droughts, with alpine grasslands showing particularly pronounced responses due to their ecological features such as shallow root depth and aggressive hydrological behavior. The Nile basin, similar to the UYR basin, exhibits pronounced late-season vegetation vulnerability, highlighting shared patterns of drought impact across heterogeneous landscapes. In contrast, the tropical rainforests in the Congo basin demonstrate greater resilience, supported by complex root systems, dense canopies, and low cloud cover that reduces evaporation. This study underscores the importance of considering regional ecological characteristics, drought timing, and phenological stages in assessing vegetation responses to drought. These insights are critical for predicting and managing ecosystem resilience under changing climatic conditions.

Plain Language Summary As climate change leads to more extreme droughts, plants are expected to struggle with growth due to water shortages. Our study investigated how vegetation in the typically humid, diverse ecosystems of the upper Yangtze River (UYR) basin responded to droughts since 2000. We found that while UYR vegetation has been affected by water stress, it may be becoming less sensitive to drought over time. Late-season droughts have a stronger negative impact on plant growth than early season ones, particularly for alpine grasslands, which are more vulnerable due to shallow roots and water use strategy. To contextualize these findings globally, we compared the UYR basin with two other major river basins: the Nile and the Congo. Similar to the UYR basin, the Nile basin exhibits significant late-season vulnerability. In contrast, the Congo basin, dominated by tropical rainforests, is more resilient to drought, buffered by complex root systems, dense canopies, and low cloud cover, which reduces evaporation. Our results highlight the importance of understanding the adaptive mechanisms that vegetation employs in response to water stress, as these mechanisms can influence ecosystem services such as carbon storage, biodiversity, and water regulation.

1. Introduction

Changes in climate-related extreme events have been observed since the 1950s, and future drought is expected to increase in frequency, intensity and duration, aggravating ecosystem vulnerability to climate variability (IPCC AR6 WGI, 2021). Evidence indicates a reduction in ecosystem resistance and resilience to drought, suggesting decreasing ecosystem stability under climate change (Yao et al., 2024). As the climate warms, vegetation growth tends to happen earlier in the season, while becoming more susceptible to water limitations at the end of the

season (Pompa-García et al., 2021). Drought-induced water deficit limits vegetation growth by reducing soil moisture and increasing evaporation demand (Aguirre et al., 2021). Simultaneously, extreme drought also increases the risk of relevant disturbances such as heat stress, fire, insects and pathogens outbreaks (Anderegg et al., 2020).

Responses of vegetation to droughts have been quantified by numerous studies; however, the effect of water deficit on vegetation growth varies enormously due to the complicated scales (i.e., temporal and spatial) and dimensions (i.e., duration, intensity, frequency and timing) of drought events (Jiao et al., 2022). Climate models predict increasing drought intensity and frequency with important consequences on vegetation growth (Lewis et al., 2011; Ma et al., 2012; Zhou et al., 2014). Vegetation sensitivity to drought has been shown to partly depend on vegetation types and associated water-regulation strategies, which are co-controlled by local environmental conditions (Anderegg, 2015; Vicente-Serrano et al., 2010). In recent decades, seasonal drought has become more frequent and intense (Song et al., 2019; Sun et al., 2016; L. Wang et al., 2015), even in regions previously regarded as abundant in precipitation and water resources. The timing of droughts and plant phenology also affect the responses of vegetation to drought (D'Orangeville et al., 2018; Foster et al., 2014; B. Xu et al., 2020), especially in the case of seasonal droughts. A study in an eastern temperate forest suggests that tree growth is most affected by early season droughts when radial growth rates are highest (D'Orangeville et al., 2018). Water availability in spring is critical for the following vegetation growth, which is associated with the process of leaf bud development and leaf unfolding (Bai et al., 2004; Zeiter et al., 2016). As long as the bud breaks, leaf development is largely influenced by water availability due to cell expansion (Brando et al., 2010). In contrast, experiments suggest that temperate grass resistance to spring drought is higher when plants are in reproductive stages and their growth rates are highest (Hahn et al., 2021). As different growth forms have different hydraulics and sensitivity and may respond differently to water availability, in general, if the plant sensitivity to drought varies across phenological phases and how the timing of drought and phenology affect vegetation growth remain unclear and understudied.

Multiple big river basins around the world are facing the threat of drought, such as the Nile River (Nigatu et al., 2024), the Amazon River (Brando et al., 2010; L. Xu et al., 2011), and rivers in the United States like the Colorado River (Bedri & Piechota, 2022) and the Mississippi River (Jiang et al., 2019). The upper Yangtze River (UYR) basin is a humid big river basin located in Southwest China, in a temperate climate zone with abundant precipitation. Radiation and temperature were previously regarded as primary climatic constraints for vegetation growth in Southwest China, rather than water availability (Nemani et al., 2003). However, recent increases in the intensity and frequency of droughts could potentially lead to the long-term water deficit becoming a key limitation on vegetation growth. Due to the large elevation gradients of more than 7,000 m across this basin, natural differences in climate factors occur, resulting in a variety of vegetation types with different hydraulics and phenology from low to high altitudes (Chuine, 2010; Cleland et al., 2007; Körner, 2007; Peñuelas et al., 2009; Piao et al., 2019). Consequently, the response pattern to drought in the UYR is anticipated to be more complex compared to other large river basins located in plains, such as the Amazon and Congo. In the face of such complexities, effective ecosystem management necessitates understanding the relative resistance and resilience of these ecosystems to global change.

Investigating important drivers and how they affect vegetation responses to drought is critically important for improving the understanding of the vegetation-climate interplay and reducing uncertainty in earth system models (Prentice et al., 2015). Here we test the role of drought timing and plant phenology on the response of vegetation growth to drought in the UYR basin along with a global comparison of big rivers. We hypothesize that (a) vegetation resistance to drought differs in their growing stages and plants are more sensitive to droughts when they are in their rapid growing stages; (b) elevation-induced differences in vegetation types and phenological metrics across the basin will lead to a diverse response pattern to droughts.

2. Materials and Methods

2.1. Study Area

The UYR originates from glacier meltwater in the Tanggula Mountains and descends to Yichang, Hubei province, with a length of 4,511 km, accounting for about 70% of the total length of the Yangtze River (Figure 1a). The Yangtze River spans an elevation gradient of 7,000 m, resulting in a sharp change in basin characteristics. Climate characteristics exhibit obvious gradients along elevation, lower altitude area shows relatively higher precipitation,
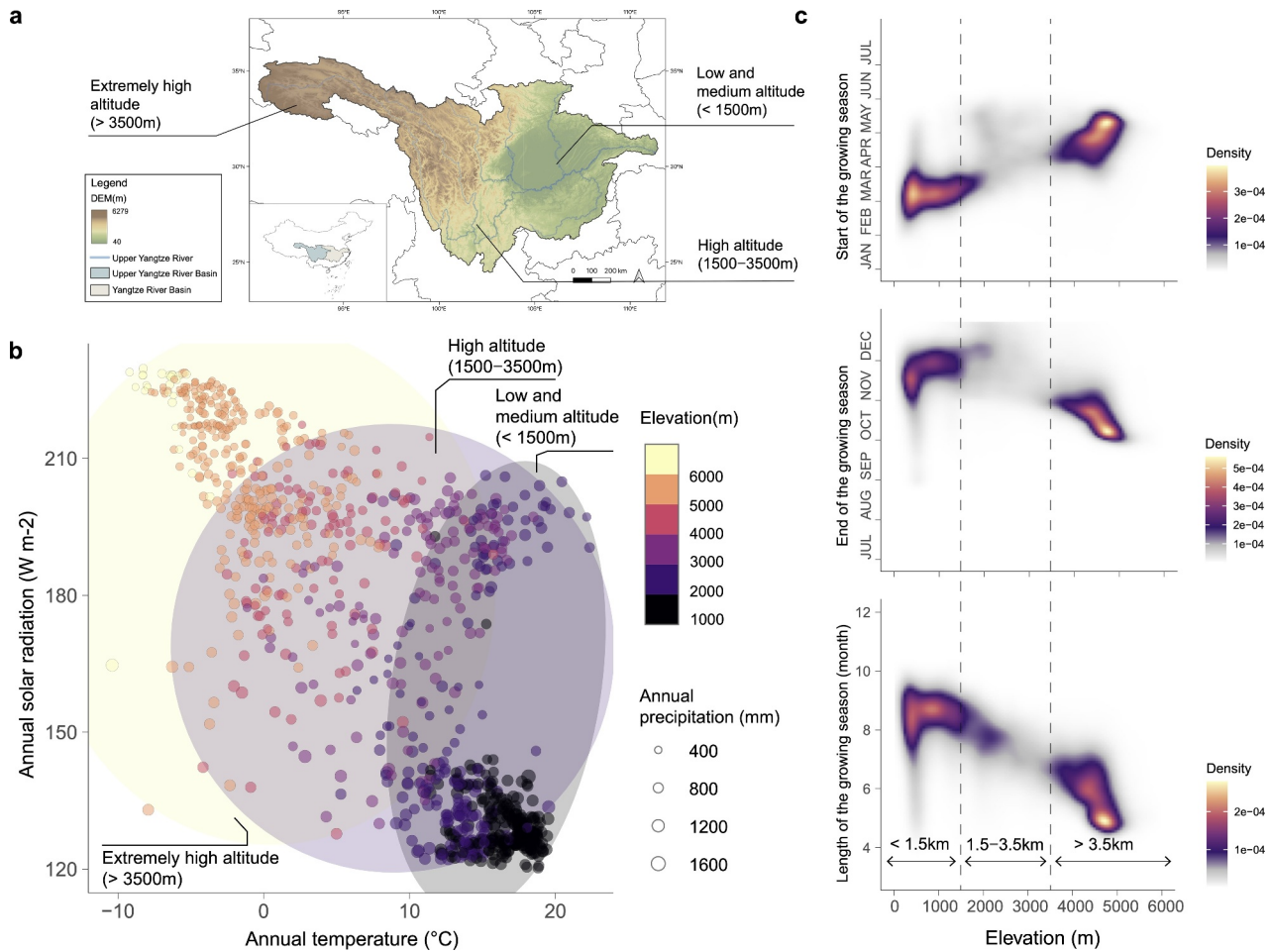
Figure 1. The characteristics of the upper Yangtze River basin. (a) The digital elevation model (DEM) of the upper Yangtze River basin. (b) The climate characteristics of the upper Yangtze River basin along elevational gradients (averaged over 2000–2018; spatial distributions see Figure S1 in Supporting Information S1). Dots are randomly sampled pixels from the study area. Shaded areas indicate three altitude gradients. (c) The relationship between phenological metrics (averaged over 2000–2018; spatial distributions see Figure S2 in Supporting Information S1) and elevations. Point density is indicated by colors. Dashed lines give the range of elevation gradients.

higher temperature, and lower solar radiation than higher altitude areas (Figure 1b). The low-altitude areas are classified as subtropical humid regions, while the high-altitude areas are classified as temperate plateau regions. Phenology metrics (start, end, and length of the growing season) are also spatially controlled by altitude due to temperature gradients over the basin (Figure 1c). According to the distributions of main climate characteristics (Figure S1 in Supporting Information S1), we split the basin into three altitude gradients: low and mid-altitude (<1,500 m, LMA); high altitude (1,500–3,500 m, HA); extremely high altitude (>3,500 m, EHA). Compared to EHA, vegetation's growing season in LMA starts earlier and ends later about 1–2 months respectively, therefore with a longer growing season than EHA (Figure 1c). Phenological metrics maps over 2000–2018 were shown in Figure S2 in Supporting Information S1. Furthermore, climatic region differences result in changes in vegetation types along the altitudinal gradient. Grasslands are almost the only vegetation present in EHA (temperate plateau regions) with a correspondingly short growing season (Figures 1c and 2). The UYR basin presents a typical forest-grassland ecotone (Figure 2). For the global comparisons to the UYR basin, we selected basins with similar characteristics to the UYR basin, known for water abundance but trending toward drying. According to the observed long-term trend of the aridity index (AI, the ratio of annual precipitation to potential evapotranspiration) reported by Huang et al. (2016), the Congo and Nile River basins have experienced a remarkable decrease in AI, similar to the UYR basin over the past few decades. Figure S3 in Supporting Information S1 shows the standard precipitation evaporation index (SPEI) series of the Congo and Nile basins for 2000–2022, highlighting severe drought events that occurred.
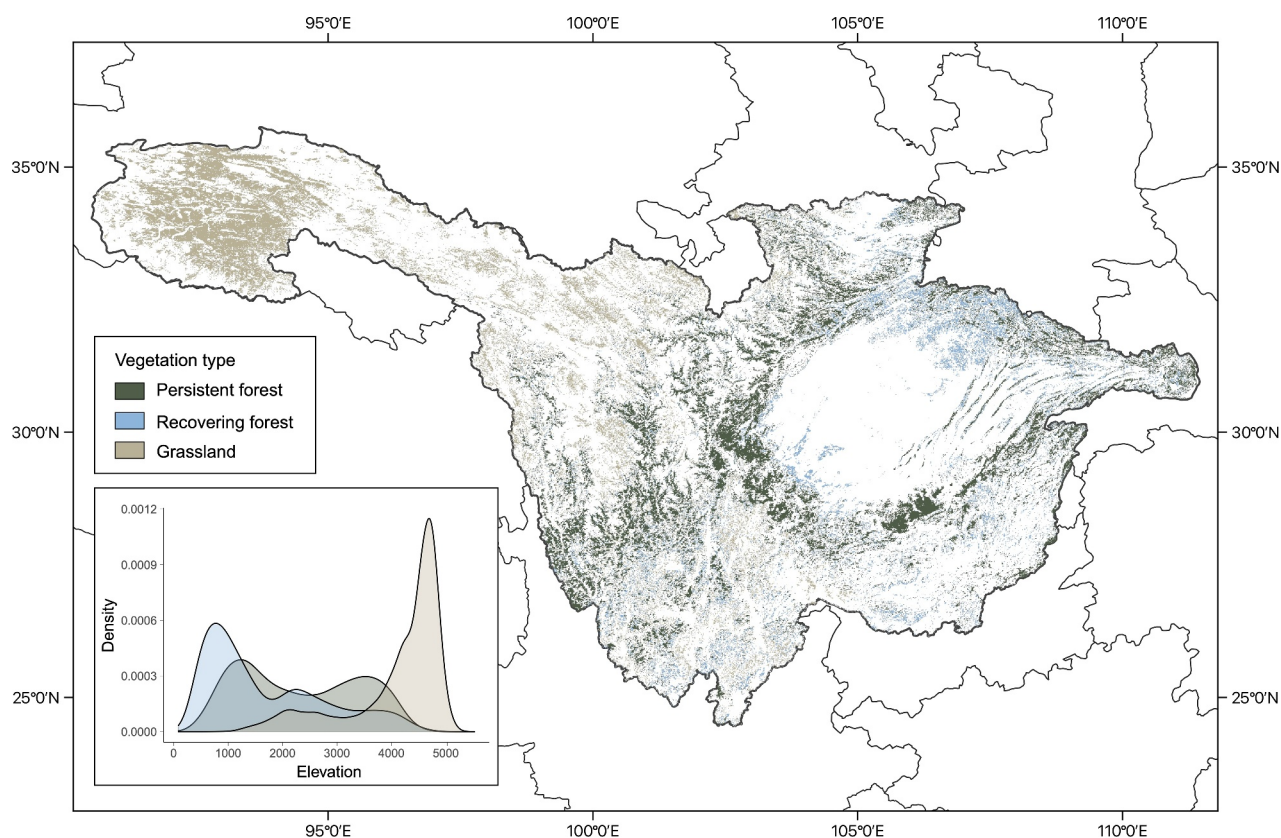
Figure 2. Vegetation types in the upper Yangtze River basin. The density plot indicates the distribution of basin vegetation along elevational gradients.

2.2. Data Collecting

Climate data used for analysis in the UYR basin were obtained from the China Meteorological Forcing Data, which offers a spatial resolution of 0.1°. This data set was chosen for its higher resolution compared to most global data sets and covers the period from 1979 to 2018. For global comparisons among big river basins, climate data were obtained from the CRU TS V4.05 data set due to the global availibility, available from the Climatic Research Unit (University of East Anglia, https://crudata.uea.ac.uk/), with a spatial resolution of 0.5°. The soil moisture data was derived from the ERA5-Land data set. This data set provides 4 vertical layers of soil moisture (0–0.07 m, 0.07–0.28 m, 0.28–1.0 m, and 1.0–2.89 m). The sum of 0–1.0 m soil moisture was used to reflect the soil moisture in forests with deep roots. The land cover map of the UYR basin is derived from the European Space Agency (ESA) Climate Change Initiative (CCI) projects. A large area of urban and mixed irrigated and rainfed cropland distributed at the low and mid-altitude of the basin was excluded from this study because it is particularly affected by human activities. We used Moderate resolution Imaging Spectroradiometer (MODIS) MOD09GA V006 surface reflectance data to classify types of vegetation and land use change. We included two vegetation indexes data sets as the proxy of vegetation growth. The Normalized Difference Vegetation Index (NDVI) product MOD13A3 V006 with a spatial resolution of 1 km. The Normalized Difference Vegetation Index (NDVI) derived from Global Inventory Modeling and Mapping Studies-3rd Generation V1.2 (GIMMS-3G+) with a spatial resolution of 1/12° degrees. MODIS NDVI was primarily used to extract the phenological metrics and quantify vegetation responses to droughts during growing stages within the UYR basin due to its high resolution, while GIMMS NDVI was used for temporal response calculation and global comparisons of major river basins. The time coverage of all data used in this study aligns with the study duration, spanning from 2000 to 2018, during which all data sets were readily available.

2.3. Drought Detection

We used the 3-month standard precipitation index (SPI), the standard precipitation evaporation index (SPEI) and the z-score of soil moisture (0–1.0 m) from its climatology ($z = \frac{X_i - \mu}{\sigma}$, where X_i is the soil moisture for the month i, μ, and σ are the mean and standard deviation of the month i from all the observation years) to identify the occurrences of seasonal droughts and their spatial distribution from 2000 to 2018. The calculation of SPEI is similar to SPI but includes a water balance (the difference between precipitation and evapotranspiration) (Vicente-Serrano et al., 2010). Potential evapotranspiration (PET) was calculated using the Penman-Monteith method (Monteith, 1965), which is widely considered the most accurate way to estimate PET. For detailed calculations of SPI, SPEI and PET see Supporting Information S1.

We defined droughts as periods when SPI and SPEI are below −1. Drought levels are classified into moderate drought (−1.5 < SPI/SPEI < −1), severe drought (−2 < SPI/SPEI < −1.5) and extreme drought (SPI/SPEI < −2) according to Mckee et al. (1993). Short-term droughts (less than 2 months) were excluded due to the potential time-lag effect of vegetation physiological drought to meteorological drought. The impact of anomalously low precipitation within 1 month may be hard to detect if soil water storage is available because vegetation can utilize deeper soil water through drought periods, especially in humid regions (Anderegg et al., 2020). Thus, the z-score of soil moisture was used to quantify the anomalies of soil moisture from the historical mean condition. Detailed calculation of the long-term trends of drought frequency and vegetation responses see Supporting Information S1.

2.4. Types of Vegetation and Land Use Change

As the large-scale vegetation restoration projects conducted over the UYR basin from 1999. To clarify vegetation responses to drought under a background of vegetation recovery, we used a similar method as Tong et al. (2020) to identify the main types of vegetation and land use change. They applied this method in almost the same study area and time periods. All calculations were based on the platform Google Earth Engine (GEE). We first created annual forest and grassland probability maps from MODIS MOD09GA V006 surface reflectance data. A total of 632 forests, 269 grasslands and 1066 non-vegetated training points were manually selected by comparing with Google images and annual ESA CCI land cover maps for 2000–2018 to train the Random Forest classifier and generate annual forest and grassland probability maps. The probability is the output of the Random Forest classification which ranges from 0 to 1 and represents the probability that the classification is correct. A probability of 0.5 is commonly used by the Random Forest classifier as a threshold to identify if a pixel belongs to a class or not, thus we used the threshold of 0.5 to identify if a pixel belongs to forest, grassland or none of them and investigate how it changed over time.

Then, we classified types of vegetation and land use change by applying Landsat-based Detection of Trends in Disturbance and Recovery (LandTrendr) to the maps of the annual probability of each classification. The LandTrendr algorithm is used to fit the annual data into segments to identify vertices (breakpoints) separating periods of durable change. The top-ranked forest type was consistently broad-leaved mixed forest, occupying the majority of the forest area in the UYR basin (Y. Wang et al., 2023). Shrublands and grasslands are also prevalent in certain areas, particularly regions with higher elevations and drier conditions. Considering the dominant vegetation types in the UYR basin, we subsequently used the annual forest and grassland probability maps for 2000–2018 to generate three classes of vegetation. The forest classes included (a) persistent forests (forest probability always ≥0.5) and (b) recovering forests (forest probability changes from non-forest (<0.5) to forest (≥0.5), without disturbances); the grassland class only includes persistent grassland (grassland probability always ≥0.5), excluding the area with snow and ice.

The geographic distribution of vegetation types over the basin is shown in Figure 2. Only a few pixels (less than 1%) changed from non-forest to forest with disturbances were detected by LandTrendr, thus we excluded those pixels from subsequent analysis. The type of recovering forest indicated a slow and gradual increase of tree cover without any disturbances which is represented by the breakpoint (vertex) in the time series of annual forest probability. Most of the restored forest areas were previously cropland or grassland, indicating the implementation of natural forest recovery or planting of slow-growing species across the UYR basin.

2.5. Vegetation Growing Dynamics

NDVI time-series data is widely applied in phenology characterization at the landscape scale (Piao et al., 2019; Zhang et al., 2003). Data smoothing is required for reducing noises such as cloud contamination, aerosols, sun-angle, sensor performance and other data errors. The extraction of phenology metrics was carried out by the dynamic threshold method (White et al., 1997) that assumes the growing season started and ended when the smoothed NDVI reaches a specific percentage of the annual amplitude $\left(\text{NDVI}_{ratio} = \frac{\text{NDVI} - \text{NDVI}_{min}}{\text{NDVI}_{max}}\right)$. Here, we defined the start and end of the season when the NDVI_{ratio} reached 0.25, which are most widely used in literature and closest to field observations (Yu et al., 2010). The phenology analysis was calculated by R package greenbrown. We used the function *TSGFspline()* to do gap-filling and data smoothing of the time series. Phenology metrics were detected by the function *PhenoTrs()*. To define the vegetation growth stages, we used a similar method from Jiao et al. (2022). We divided the growing season into the early season for NDVI increasing period, and the late season for NDVI decreasing period. Stages outside the growing season are referred to as "out of season." Then, the vegetation growth stages were divided in detail by percentage of NDVI_{ratio}.

The drought impact on vegetation growth is represented by the deviation from drought years relative to the mean of the reference period (Wolf et al., 2016). Since the implementation of large-scale vegetation restoration projects over the UYR basin since 1999, vegetation cover has shown a general greening trend since 2000, which may introduce confounding factors when calculating drought responses. Therefore, we used STL (Seasonal-Trend decomposition using LOESS) to decompose and remove the long-term greenness trend starting from 2000 (Cleveland et al., 1990). STL is a robust and flexible method for time series decomposition, as it can effectively separate seasonal, trend, and remainder components without requiring prior assumptions about the data's structure:

$$\text{NDVI}(t) = T(t) + S(t) + R(t),$$

where

$\quad$ $\text{NDVI}(t)$ is the original NDVI series,
$\quad$ $T(t)$ is the trend component, representing long-term changes,
$\quad$ $S(t)$ is the seasonal component, capturing periodic patterns,
$\quad$ $R(t)$ is the remainder (residual) component, which includes random variations and noise.

STL uses LOESS smoothing iteratively to estimate the trend and seasonal components. Its flexibility allows for the adjustment of smoothing parameters to adapt to diverse time series structures, making it particularly effective for handling complex patterns in data, such as vegetation indexes. Notably, STL can manage data containing missing values and is resistant to distortions from outliers or abrupt changes. In our analysis, after decomposing the time series, we extracted and removed the trend component $T(t)$ to produce detrended data:

$$\text{NDVI}_{detrended}(t) = \text{NDVI}(t) - T(t)$$

The z-score of the detrended NDVI was used to represent the anomaly in vegetation growth. Since NDVI exhibits significant seasonality, calculating anomalies using the mean if all months would be affected by seasonal fluctuations. To address this issue, we removed the seasonal component $S(t)$, specifically the mean of the same month across all years, before calculating the anomalies:

$$\text{NDVI Anomaly} = \frac{\text{NDVI}_{detrended, deseasonalized}(t) - \mu}{\sigma},$$

where μ and σ are the mean and standard deviation of the detrended and deseasonalized NDVI series. This step ensures that the calculated anomalies accurately reflect deviations independent of seasonal patterns.

The implementation was performed using the *stl()* function from the R package forecast. To ensure methodological consistency throughout the study, we applied this method uniformly to the NDVI anomaly calculations across all basins, thereby enhancing the comparability of results among them.
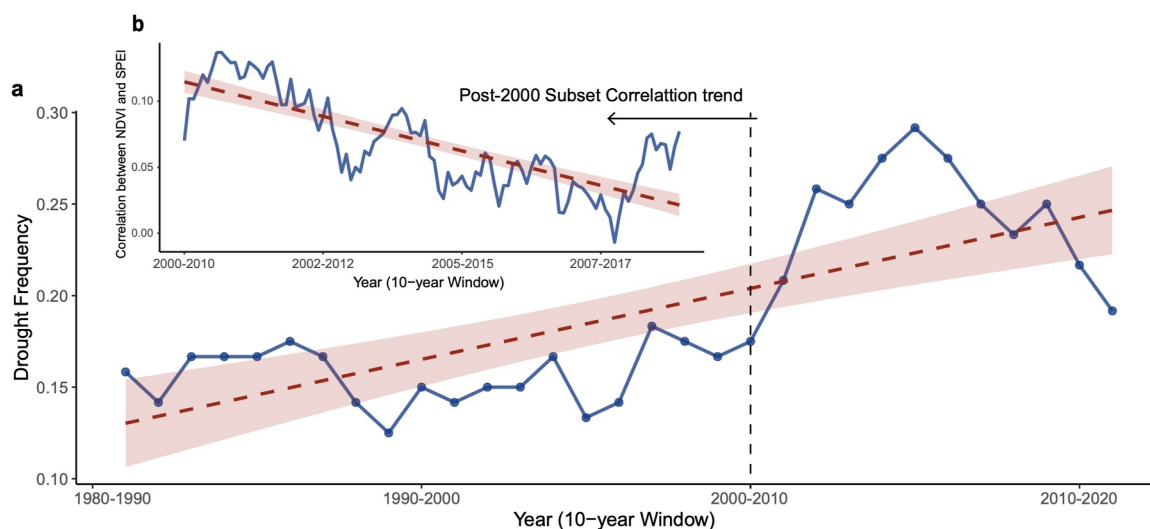
Figure 3. Trends in drought frequency and vegetation growth-drought correlation over time in the UYR Basin. (a) Drought frequency from 1980 with a 10-year moving average. (b) Spearman correlation between vegetation index (NDVI) and drought index (SPEI) from 2000 with a 10-year moving average. Drought frequency indicates the number of months in a 10-year moving window with the SPEI below −1.

Additionally, only pixels that detected droughts (with SPI or SPEI falling below −1) for at least 3 months were included in the calculations to avoid confounding effects from non-drought areas and short-term droughts.

3. Results

3.1. Increased Drought Frequency Since 2000

By analyzing the drought frequency trend over the past four decades, we observed a marked increase in drought occurrences around the year 2000 with a significant upward trend in the 10-year moving average during 1980–2020 (Figure 3a, Mann-Kendall trend test: $z = 3.85$, $p < 0.001$). Consequently, we focus on the period after 2000, as the UYR basin experienced a sudden rise in drought occurrences that remained elevated compared to earlier periods.

Figure 3b examines the correlation between vegetation NDVI and SPEI since 2000, revealing a consistent positive correlation that suggests vegetation growth is responsive to drought conditions, with drought exerting a suppressive impact on vegetation growth. However, a downward trend in the vegetation-drought correlation was observed (Mann-Kendall trend test: $z = -8.66$, $p < 0.001$), indicating that vegetation is becoming less sensitive to drought. This reduced sensitivity could be attributed to potential acclimation, the buffering effect of species diversity in humid regions mitigated the increasing trend in sensitivity to water stress (Liu et al., 2025). Figure 4 provides further insight into drought variability since 2000, utilizing different drought indicators (SPEI and SPI). Five drought events were captured by both SPEI and SPI, particularly with significant dry spells from 2009 to 2013. Figure 4c highlights soil moisture anomalies, showing changes in water availability at the 0–1 m layer that align with the drought periods indicated in SPEI and SPI. Together, these indexes offer a comprehensive view of drought variability in the UYR basin, with certain years marked by pronounced moisture deficits affecting both precipitation levels and soil water content.

3.2. Seasonal Response Patterns of Vegetation Growth to Droughts

The drought events observed since 2000 generally last 1 to 2 seasons (Figure 4). To understand the temporal responses of vegetation to drought, we divided the year into early and late growing seasons and out-of-growing seasons based on vegetation phenology. The significant elevation differences across the UYR basin lead to gradients in varying vegetation types and phenology (Figures 1 and 2), with alpine grasslands having a shorter 6-month growing season compared to the 8-month growing season of forests, although both peak in NDVI in August (Figures 5a and 5b).
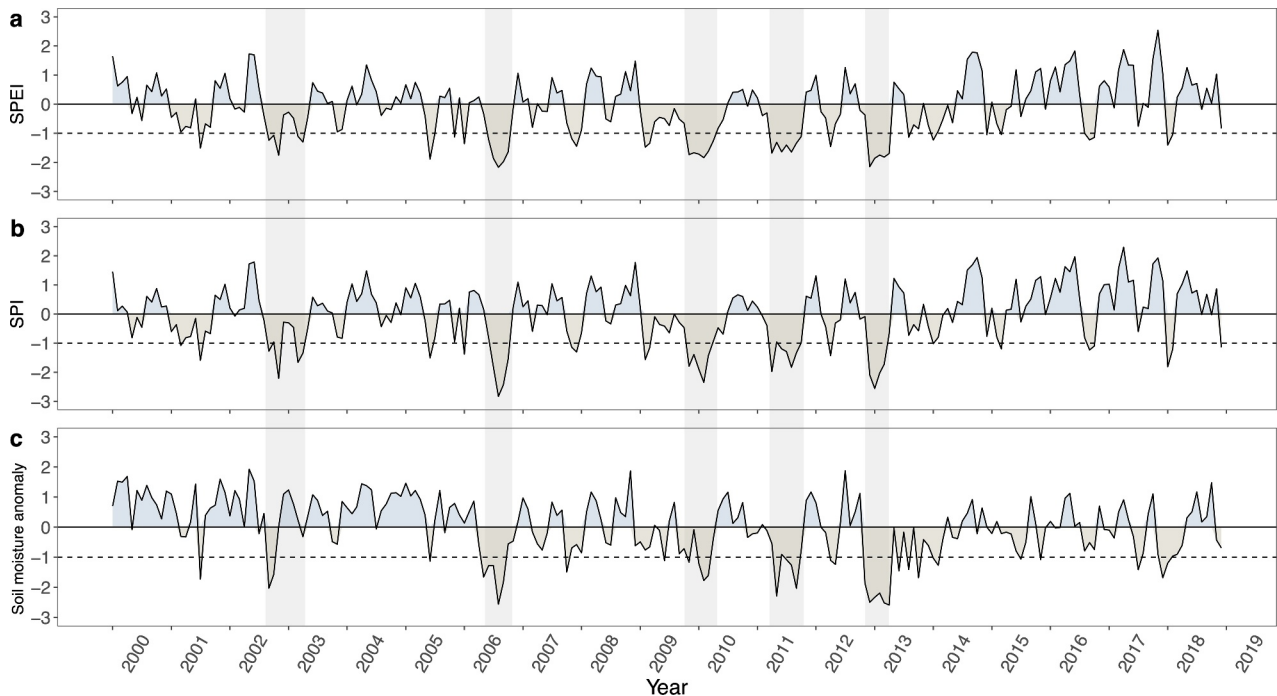
Figure 4. Drought indexes from 2000 to 2018. (a) SPEI. (b) SPI. (c) Soil moisture anomaly. Shaded areas indicate the period of droughts.

NDVI anomalies reflect how different vegetation types responded to drought, exhibiting distinct seasonal patterns (Figures 5d and 5e). Persistent forests generally show more resilience to drought across the seasons, maintaining relatively stable NDVI anomalies. Recovering forests, and particularly grasslands, exhibit pronounced declines during drought periods. For instance, the late-season drought of 2002 resulted in significant NDVI drops in alpine grasslands. Moreover, vegetation in the UYR basin shows varying sensitivities to drought depending on the timing within the growing season. Early season droughts, such as those in 2006 and 2011, had minimal impacts on NDVI across vegetation types. Similarly, out-of-season droughts (e.g., 2003, 2012–2013) had no negative effect, as most plants were dormant and less reliant on water availability. In contrast, late-season droughts consistently led to substantial declines. For example, during the 2006 drought, NDVI began to decrease as vegetation transitioned to the late growing season, recovering to normal conditions after the drought ended. A similar pattern was observed during the 2011 drought, with a sudden decrease in NDVI during the late season. However, the 2009–2010 drought, which spanned late 2009 and early 2010, caused NDVI declines in both growing seasons. This may be due to the significant depletion of water by the late-season drought in 2009, followed by a continued lack of rainfall replenishment—unlike the 2002–2003 drought—resulting in lagged impacts on early season growth the following year.

To further investigate how vegetation phenology and drought timing modulate drought impacts, we analyzed vegetation responses across different growth stages for each vegetation type. Persistent forests were almost unaffected by drought during the entire season (Figure 6a), while recovering forests were slightly impacted by extreme drought during the early growing stage, reflected by an NDVI ratio of 20%–60% (Figure 6b). Compared to forests, grasslands are more vulnerable to drought overall. Specifically, moderate impacts on grasslands were observed during the early growing stage when NDVI ratios ranged from 20% to 80%. Pronounced negative impacts on grasslands occurred during the late season, with NDVI ratios declining from 70% to 30% (Figure 6c). Severe and extreme droughts had a greater impact on grasslands than moderate droughts, with mean negative NDVI anomalies reaching as low as −1.29 (Figure 6c). Additionally, droughts had no or minimal impacts when either forests or grasslands were in their growing or peak photosynthetic periods.
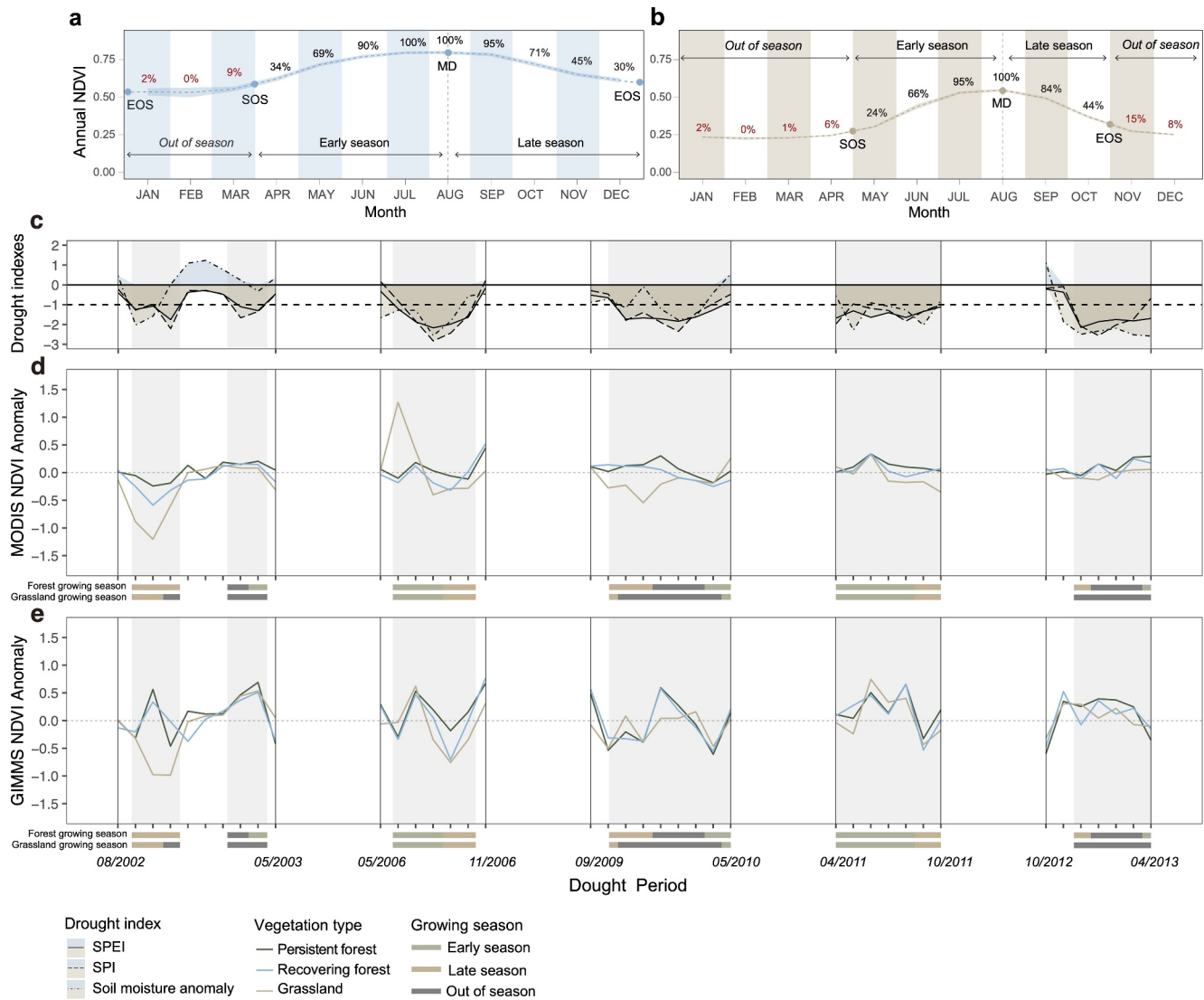
Figure 5. Vegetation responses to detected drought events among persistent forest, recovering forest and grassland. (a, b) Annual Normalized Difference Vegetation Index (NDVI) shows the growing curve of a forest and b grassland. Percentages indicate the $NDVI_{ratio}$. Red percentages indicate months out of the growing season ($NDVI_{ratio} < 25\%$). (c) Drought index for drought events. (d) Anomalies of MODIS NDVI. (e) Anomalies of GIMMS NDVI. Shaded areas indicate the period of droughts. Bars below the *x*-axis indicate the growing seasons of forest and grassland.

3.3. Comparisons With Other Humid Big River Basins Suffering Droughts

Given the unique characteristics of the UYR basin, including substantial elevation differences, a humid climate with recurrent droughts, and large-scale vegetation restoration efforts, we identified comparable basins that share similar conditions—abundant water resources yet frequent drought events in recent years. Our analysis aims to investigate whether these basins exhibit seasonal patterns of drought response similar to those observed in the UYR basin. The Congo and Nile basins serve as vital reservoirs of freshwater resources for Africa. Although these basins benefit from abundant rainfall, particularly in their equatorial regions, they have experienced up to 20 drought events in the past four decades, characterized by prolonged dry spells and erratic precipitation patterns linked to climate change (Figure 7g and Figure S3 in Supporting Information S1). Figure 7 shows the GIMMS NDVI responses to both early season and late-season droughts in these basins. Late-season droughts generally have large negative impacts in the Nile basin, similar to those found in the UYR basin (Figures 7a–7d). In contrast, this pattern was not observed in the Congo basin (Figures 7e and 7f). Both early- and late-season droughts in the Congo Basin showed no significant differences in their impacts, with both resulting in a mean NDVI anomaly around 0 (Figure 7f), indicating no distinct vegetation response to drought.
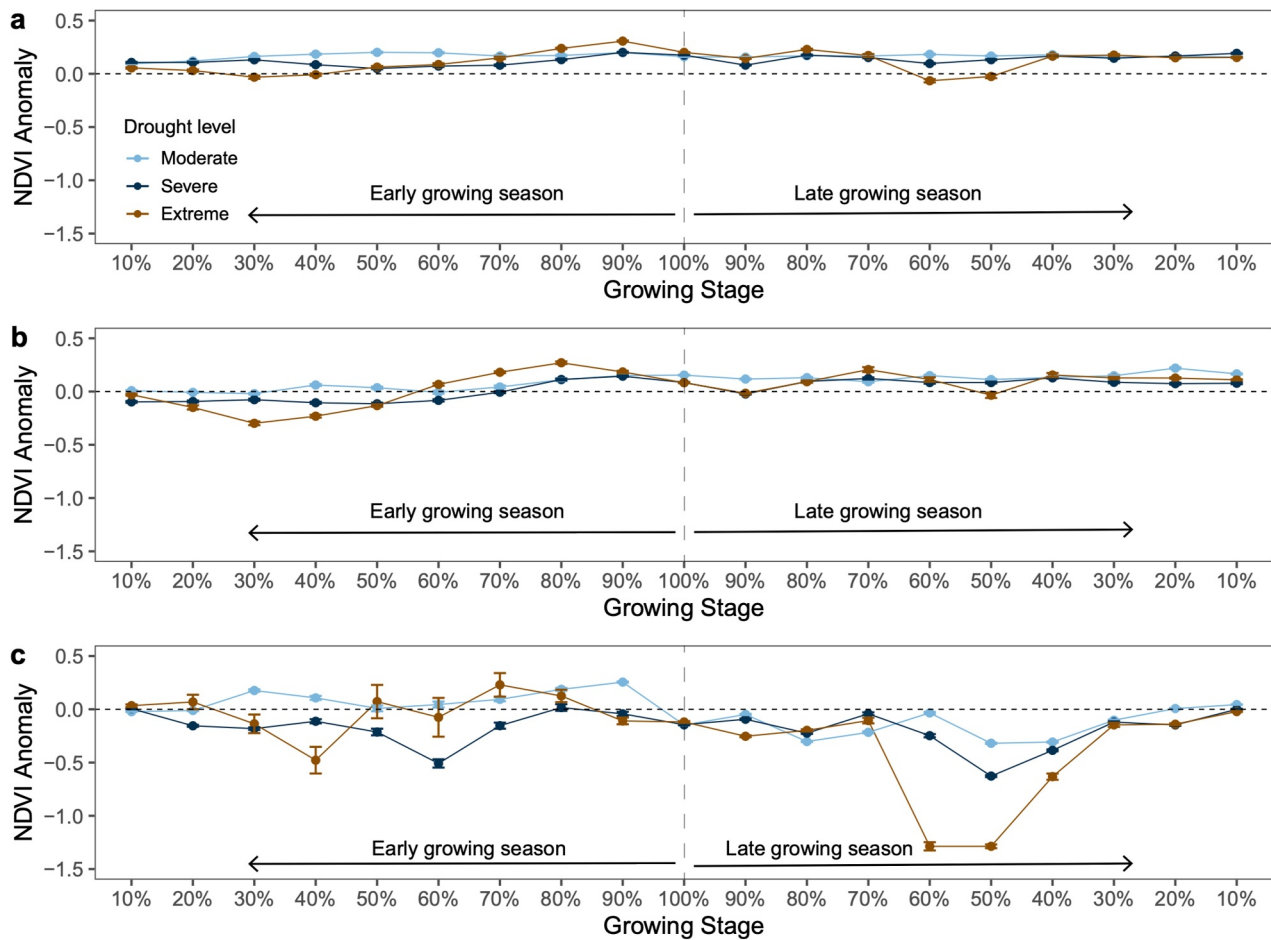
Figure 6. Vegetation responses to drought along growing stages. Vegetation responses to drought along growing stages are indicated by the differences in NDVI anomaly. (a) Persistent forest, (b) recovering forest and (c) grassland.

4. Discussion

4.1. Heterogeneous Responses of Humid UYR Basin to Drought

In contrast to arid ecosystems, the understanding of drought impacts on humid ecosystems is very limited because water deficits are not usually regarded as the main factors limiting vegetation growth. Humid ecosystems, such as the UYR basin, play a critical role in carbon storage and biodiversity. However, this basin experienced a sharp increase in drought frequency in 2000, leading to sustained water deficits in certain years (Figures 3 and 4). This raises concerns about the potential vulnerability of humid biomes, as they are generally less adaptable to water stress compared to arid biomes, which have evolved flexible physiological water-use strategies (McDowell et al., 2008). Such strategies include (a) increasing internal water content to avoid tissue damage (McDowell et al., 2008) or (b) sustaining low internal water content to maintain growth during drought periods (Gupta et al., 2020). Our study revealed that vegetation in the UYR basin has become less sensitive to increasing drought stress, as evidenced by a declining trend in the vegetation-drought correlation since 2000 (Figure 3b). Forests, particularly persistent forests, displayed considerable resistance to drought (Figures 5 and 6). This resilience in persistent forests may be attributable to the temporary depletion of moisture in the upper soil layers (0–1 m) driven by seasonal droughts, which can quickly recover to normal levels once the drought subsides (Figure 4c). Additionally, if sufficient subsoil water reserves exist, they can buffer vegetation growth against precipitation variability, since meteorological droughts (e.g., SPI and SPEI anomalies) have limited direct effects on vegetation under such conditions (Elliott et al., 2006).

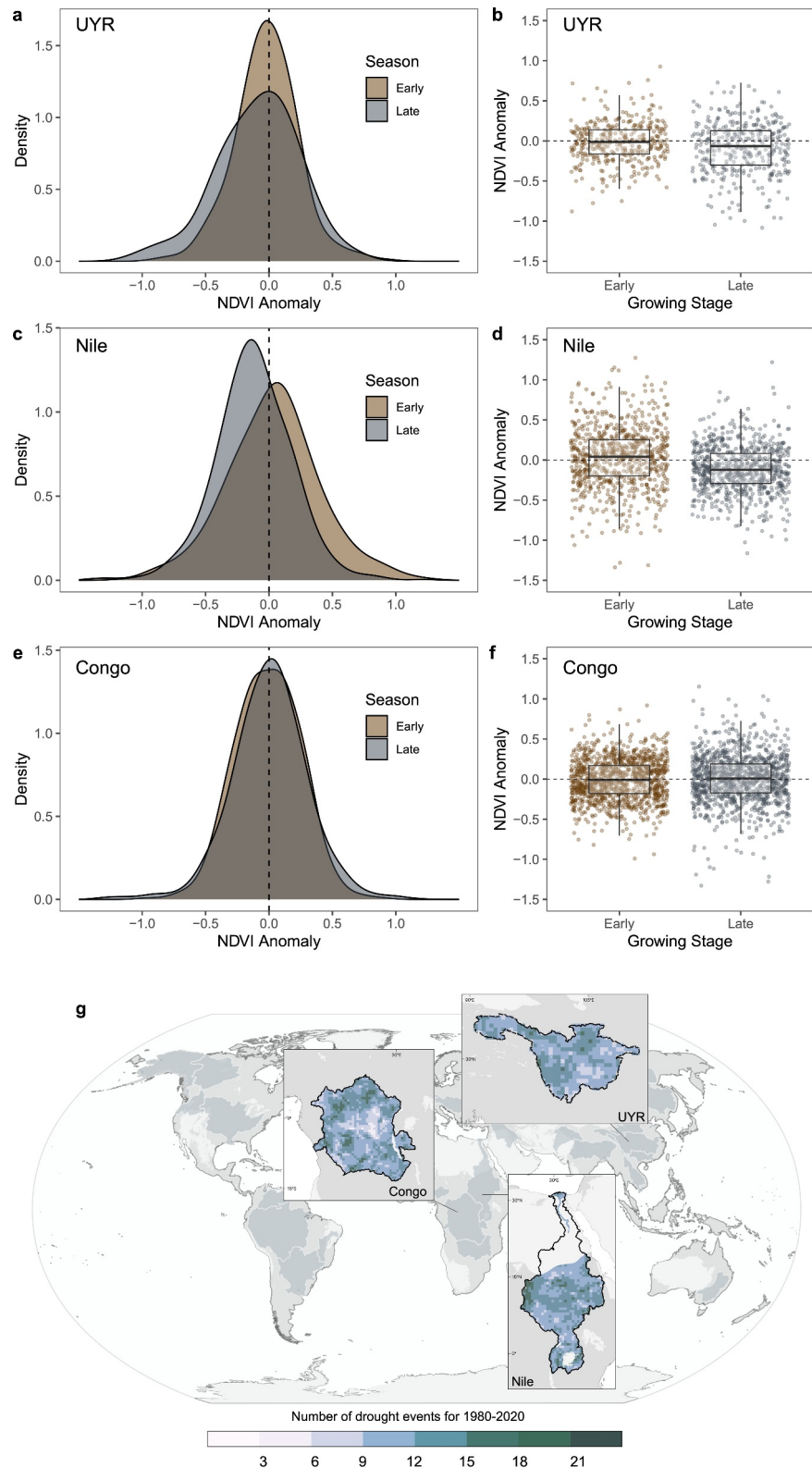**Figure 7.** Comparison of global humid big river basins prone to frequent droughts. Vegetation responses to early- and late-season drought in (a, b) the upper Yangtze River basin, (c, d) Nile basin and (e, f) Congo basin. (g) Map showing the frequency of drought occurrences for 1980–2020 in the upper Yangtze River, Nile and Congo basins. Drought events were identified as SPEI below −1 continued for at least 3 months.

In contrast, recovering forests are relatively more vulnerable, likely due to their less stable ecological structure and reduced resilience to environmental stressors. This instability may arise from factors such as younger age, lower biomass, or less developed root systems, which render them less equipped to withstand drought and other adverse conditions (Anderson-Teixeira et al., 2013). Despite this resilience, we observed that forest responses to drought are subtle and vary across seasons (Figure 5). The visible effects of drought may not always be immediately reflected in forest appearances, as indicated by remote sensing data (Mallick et al., 2016). Nonetheless, physiological changes, such as surface conductance, are significant even if they are not detectable by remote sensing, and these effects may become evident in growth and leaf area in the following year (Anderegg et al., 2015; Hoek van Dijke et al., 2023; Senf & Seidl, 2021). For example, during the prolonged drought spanning two growing seasons in 2009–2010, we observed that the effects of the late-season drought in 2009 likely extended into the early season of 2010, resulting in a visible decline in forest NDVI (Figure 5). This decline was not observed with early season droughts following non-drought years, such as those in 2006 and 2011 (Figure 5).

While forests show varying degrees of resilience to drought, grasslands—particularly those in high-altitude areas—exhibit distinct patterns of drought response. Grasslands demonstrate greater negative responses to drought in terms of their temporal responses (Figure 5) and anomalies across growing stages (Figure 6). Compared to trees, which adopt conservative strategies to minimize water loss by regulating stomatal conductance and reducing the risk of aboveground biomass loss (Wolf et al., 2013), grasses sustain high photosynthesis and transpiration rates with less strict stomatal control, leading to wilting and a decline in green biomass during droughts (Zha et al., 2010). Moreover, alpine grasslands are more significantly affected by drought due to low annual precipitation and recover more slowly than lowland grasslands because of shorter growing seasons and the challenges of seed establishment in these harsh conditions (De Boeck et al., 2018).

4.2. Seasonal Dynamics of Vegetation Responses to Drought in the UYR Basin

The timing of drought significantly influences its impact on vegetation in the UYR basin, as reflected in NDVI anomaly patterns across growing seasons and stages (Figures 5 and 6). During the humid season, the abundance of precipitation generally sustains vegetation growth, although grasslands in high-altitude areas remain more susceptible to drought. Data from the Pingshan hydrological station indicate that the bulk of precipitation in the UYR basin occurs between June and September, with a mean monthly rainfall exceeding 100 mm (Gemmer et al., 2008). During this humid season, sufficient absolute soil moisture remains available for vegetation, despite the detection of relative drought. The peak rainfall period coincides with the peak growth of forests, which exhibit the most abundant foliage (Figure 5a; $NDVI_{ratio}$ of 90%–100%–95%), coinciding with the majority of the grassland growing season (Figure 5b; $NDVI_{ratio}$ of 66%–100%–84%). During the humid season, forests remained unaffected, while grasslands experienced only minor impacts (Figure 6). This pattern can be explained by the location of grasslands in high-altitude areas, which naturally receive less rainfall compared to lowland forested regions (Figure 1; Figure S1 in Supporting Information S1). Consequently, even droughts occurring during the humid season can lead to soil water scarcity in alpine grasslands. Although the humid season supports vegetation growth, the effects of drought outside this period vary significantly based on timing and vegetation type.

Droughts occurring outside the humid season exhibit contrasting impacts on vegetation, with late-season droughts generally causing more severe declines in NDVI than early season droughts (Figure 5). The limited impact of early season droughts may be due to high drought resistance during the active growth phase, as well as rapid growth rates that compensate for short-term water deficits. Previous studies have identified contrasting NDVI anomalies between early and late seasons, indicating a seasonal compensation effect from warm springs (Angert et al., 2005; Bastos et al., 2020; Buermann et al., 2018; Smith et al., 2020; S. Wang et al., 2020; Wolf et al., 2016), and enhanced vegetation activity and carbon uptake by high temperatures (Keenan et al., 2014). As vegetation transitions from peak growth to the late season, growth rates decline, and the combined negative impacts of water and temperature stresses can rapidly lead to a reduction in NDVI (De Boeck et al., 2010). In the UYR basin, the peak growing stage coincides with the highest temperatures of the year. Upon entering the late season, high temperatures continue to accelerate soil water depletion through increased evaporative demand (McDowell et al., 2008). Humid biomes are considered more sensitive to atmospheric evaporative demand because they reduce stomatal conductance when water availability in the soil and atmosphere is limited in order to maintain leaf water potentials despite drought (McDowell et al., 2008). Hence, increased evaporative demand can lead to stomatal closure, resulting in diminished carbon assimilation rates and lower reserves of non-structural

carbohydrates (Arnone et al., 2008). Furthermore, carbon starvation occurs when reserves of carbohydrates are higher in the early season for growth, and the overconsumption of resources extends the effects of drought from early to later in the season. The negative impacts of late-season droughts are exacerbated by the depletion of stored soil water for growth during earlier seasons (Lian et al., 2020). Therefore, the cumulative effects of both early and late-season droughts on plant cover exceed those of individual treatments (Bates et al., 2006).

Specifically, grasslands, which are most affected by late-season droughts, exhibit aggressive water-use behaviour and shallow root systems. This leads to rapid depletion of surface soil moisture, even under limited rainfall conditions, prioritizing high evapotranspiration over aboveground biomass (Hoek van Dijke et al., 2023). Unlike spring droughts (Mar to May), late summer droughts (Aug to Oct) have a more pronounced effect on soil moisture depletion and a greater reduction in the number of reproductive shoots of grasses (Zeiter et al., 2016). The adverse impacts of late summer droughts diminish with increased rooting depth, particularly for shallow-rooted graminoids, which consistently display high vulnerability to late summer drought (Zeiter et al., 2016). A reduction in grassland coverage during late-season droughts may contribute to diminished soil seed reserves in subsequent years (Dudney et al., 2017; Zeiter et al., 2016), potentially influencing plant abundance despite forthcoming precipitation. In addition, grasslands in the source region of the Yangtze River have experienced permafrost degradation as a result of climate change (Immerzeel et al., 2010). The increased duration of soil thaw may have disrupted the stability of permafrost in this region, which, in turn, adversely affects vegetation growth by exacerbating water stress throughout the growing season (T. Wang et al., 2022). Permafrost degradation can enhance water infiltration and lead to dryness in the surface soil, leaving shallow-rooted plateau vegetation without sufficient moisture (M. Yang et al., 2010). Consequently, surface soil desiccation caused by permafrost degradation, along with persistent water deficits that intensify from early to late season, significantly impacts shallow-rooted plateau grasses in a changing climate.

4.3. Comparison With Global Big River Basins

To provide a broader context for understanding the findings of this study, we extended our analysis to global river basins with varying topography and vegetation compositions. The Congo and Nile basins were specifically selected for comparison, as they represent humid regions that have experienced frequent droughts (Figure S3 in Supporting Information S1; Figure 7g). A similar seasonal pattern of vegetation response was observed in the Nile basin but was absent in the Congo basin. In the Nile basin, vegetation cover exhibits a greater extent and more severe reduction during late-season droughts (Figures 7c and 7d). However, in the Congo basin, both early and late-season droughts did not lead to remarkable negative impacts (Figures 7e and 7f). These contrasting responses can be attributed to differences in climatology, topography, and vegetation composition between the two basins.

The Nile basin spans diverse landscapes and climates, supporting a rich variety of vegetation types. In the upstream region of Ethiopia, where rainfall is relatively abundant, lush forests and woodlands dominate. However, as the river flows northward through Sudan and Egypt into arid zones, vegetation shifts to drought-tolerant shrubs and grasses adapted to semi-arid and desert conditions. Similar to the UYR basin, this topographical and climatic heterogeneity creates a gradient of vegetation compositions. In the Nile basin, species in the northern regions are particularly vulnerable to water stress during late-season droughts due to their reliance on shallow root systems and high water-use strategies (Hahn et al., 2021; Nogueira et al., 2017; Zeiter et al., 2016), mirroring the UYR's pattern of vegetation vulnerability shaped by its environmental gradients.

In contrast, the predominantly lowland plains in the central Congo basin are covered by tropical rainforests with dense canopies of semi-evergreen trees and exceptionally high species diversity. The impact of drought in the central Congo basin is mitigated by the ability of the rainforest to buffer water stress through its complex root systems and canopy structures, providing greater tolerance to short-term reductions in rainfall (Asefi-Najafabady & Saatchi, 2013; Malhi & Wright, 2004). Frequent low cloud cover in this region reduces solar radiation and potential evapotranspiration, further buffering the impact of drought (Malhi & Wright, 2004). Previous research suggests that forests on low-lying alluvial terraces are largely unaffected by drought, whereas forests on slopes and plateaus experience more pronounced impacts (Silva et al., 2013). Only fragmented northern Congo Basin landscapes exhibited widespread canopy disturbances during extreme droughts, and these effects were confined to the duration of the water deficit (Asefi-Najafabady & Saatchi, 2013).

The different responses of the Nile and Congo basins underscore the critical roles of vegetation composition, topography, and climatology in shaping ecosystem resilience to seasonal droughts. While the Nile basin exhibits

varying vulnerability levels across regions, the relatively uniform tropical rainforest cover of the Congo basin provides greater stability, even under water deficit conditions.

5. Conclusions

Contrary to the common belief that humid ecosystems are well-protected from drought stress, our study highlights a sharp increase in drought frequency in the UYR basin around 2000, significantly deviating from previously established norms. Vegetation in the UYR basin has become less sensitive to escalating drought conditions, as evidenced by a declining correlation between vegetation growth and drought from 2000 to 2018. Specifically, persistent forests demonstrated considerable resistance to drought throughout the growing season, while recovering forests and grasslands, particularly alpine grasslands, were more vulnerable due to unstable ecological structures and shallow root systems. The timing of drought within the growing season plays a critical role, with late-season droughts leading to more pronounced declines in NDVI due to compounded water deficits. Furthermore, a comparative analysis with other documented humid river basins, such as the Congo and Nile basins, reveals distinct patterns: unlike the Congo's tropical rainforests, which maintain stability even during drought, the ecosystems of the UYR basin exhibit clear susceptibility, warranting urgent conservation measures as climate change progresses.

Ultimately, our research underscores that as we confront a future with more frequent and intense droughts, characteristics once deemed protective in humid ecosystems may no longer suffice. Understanding the nuanced responses of various ecosystem types to drought will be of prime importance for maintaining biodiversity and essential ecosystem services. The implications of our findings extend beyond the UYR basin, advocating for a reevaluation of ecological resilience in the face of climate extremes and calling for urgent action to safeguard vulnerable ecosystems globally.

Conflict of Interest

The authors declare no conflicts of interest relevant to this study.

Data Availability Statement

The China Meteorological Forcing Data set (CMFD) was obtained from National Tibetan Plateau Data Center Yang et al. (2015). CRU Climate data sets are available in Harris et al. (2020). MODIS products (MOD09GA, MOD13A3) are available in https://ladsweb.modaps.eosdis.nasa.gov/search/. Global GIMMS NDVI3g data set is available in Pinzon et al. (2023). ERA5-Land soil moisture data is available in Muñoz Sabater (2019). ESA CCI land cover maps are available in Defourny et al. (2023). Random forest classification for generating forest probability and land use change detection was conducted on Google Earth Engine, codes are available at https://code.earthengine.google.com/8b3aeeae8e419748ad0c652a54f8d15f. More information on LandTrendr is available in Kennedy et al. (2018). R codes for SPI/SPEI calculation, drought condition and trend analysis, NDVI anomaly calculation, and vegetation phenology metrics extraction can be found in Xiao (2025).

References

Aguirre, B. A., Hsieh, B., Watson, S. J., & Wright, A. J. (2021). The experimental manipulation of atmospheric drought: Teasing out the role of microclimate in biodiversity experiments. *Journal of Ecology*, *109*(5), 1986–1999. https://doi.org/10.1111/1365-2745.13595

Anderegg, W. R. L. (2015). Spatial and temporal variation in plant hydraulic traits and their relevance for climate change impacts on vegetation. *New Phytologist*, *205*(3), 1008–1014. https://doi.org/10.1111/nph.12907

Anderegg, W. R. L., Schwalm, C., Biondi, F., Camarero, J. J., Koch, G., Litvak, M., et al. (2015). Pervasive drought legacies in forest ecosystems and their implications for carbon cycle models. *Science*, *349*(6247), 528–532. https://doi.org/10.1126/science.aab1833

Anderegg, W. R. L., Trugman, A. T., Badgley, G., Anderson, C. M., Bartuska, A., Ciais, P., et al. (2020). Climate-driven risks to the climate mitigation potential of forests. *Science*, *368*(6497). https://doi.org/10.1126/science.aaz7005

Anderson-Teixeira, K. J., Miller, A. D., Mohan, J. E., Hudiburg, T. W., Duval, B. D., & DeLucia, E. H. (2013). Altered dynamics of forest recovery under a changing climate. *Global Change Biology*. https://doi.org/10.1111/gcb.12194

Angert, A., Biraud, S., Bonfils, C., Henning, C. C., Buermann, W., Pinzon, J., et al. (2005). Drier summers cancel out the CO_2 uptake enhancement induced by warmer springs. *Proceedings of the National Academy of Sciences of the United States of America*, *102*(31), 10823–10827. https://doi.org/10.1073/pnas.0501647102

Arnone, J. A., Verburg, P. S. J., Johnson, D. W., Larsen, J. D., Jasoni, R. L., Lucchesi, A. J., et al. (2008). Prolonged suppression of ecosystem carbon dioxide uptake after an anomalously warm year. *Nature*, *455*(7211), 383–386. https://doi.org/10.1038/nature07296

Asefi-Najafabady, S., & Saatchi, S. (2013). Response of African humid tropical forests to recent rainfall anomalies. *Philosophical Transactions of the Royal Society B: Biological Sciences*, *368*(1625), 20120306. https://doi.org/10.1098/rstb.2012.0306

Bai, Y., Han, X., Wu, J., Chen, Z., & Li, L. (2004). Ecosystem stability and compensatory effects in the Inner Mongolia grassland. *Nature*, *431*(7005), 181–184. https://doi.org/10.1038/nature02850

Bastos, A., Ciais, P., Friedlingstein, P., Sitch, S., Pongratz, J., Fan, L., et al. (2020). Direct and seasonal legacy effects of the 2018 heat wave and drought on European ecosystem productivity. *Science Advances*, *6*(24). https://doi.org/10.1126/sciadv.aba2724

Bates, J. D., Svejcar, T., Miller, R. F., & Angell, R. A. (2006). The effects of precipitation timing on sagebrush steppe vegetation. *Journal of Arid Environments*, *64*(4), 670–697. https://doi.org/10.1016/j.jaridenv.2005.06.026

Bedri, R., & Piechota, T. (2022). Future Colorado River basin drought and surplus. *Hydrology*, *9*(12), 227. https://doi.org/10.3390/hydrology9120227

Brando, P. M., Goetz, S. J., Baccini, A., Nepstad, D. C., Beck, P. S. A., & Christman, M. C. (2010). Seasonal and interannual variability of climate and vegetation indices across the Amazon. *Proceedings of the National Academy of Sciences of the United States of America*, *107*(33), 14685–14690. https://doi.org/10.1073/pnas.0908741107

Buermann, W., Forkel, M., O'Sullivan, M., Sitch, S., Friedlingstein, P., Haverd, V., et al. (2018). Widespread seasonal compensation effects of spring warming on northern plant productivity. *Nature*, *562*(7725), 110–114. https://doi.org/10.1038/s41586-018-0555-7

Chuine, I. (2010). Why does phenology drive species distribution? *Philosophical Transactions of the Royal Society B: Biological Sciences*, *365*(1555), 3149–3160. https://doi.org/10.1098/rstb.2010.0142

Cleland, E. E., Chuine, I., Menzel, A., Mooney, H. A., & Schwartz, M. D. (2007). Shifting plant phenology in response to global change. *Trends in Ecology & Evolution*, *22*(7), 357–365. https://doi.org/10.1016/j.tree.2007.04.003

Cleveland, R. B., Cleveland, W. S., McRae, J. E., & Terpenning, I. (1990). STL: A seasonal-trend decomposition procedure based on loess (with discussion). *Journal of Official Statistics*, *6*.

De Boeck, H. J., Dreesen, F. E., Janssens, I. A., & Nijs, I. (2010). Climatic characteristics of heat waves and their simulation in plant experiments. *Global Change Biology*, *16*(7), 1992–2000. https://doi.org/10.1111/j.1365-2486.2009.02049.x

De Boeck, H. J., Hiltbrunner, E., Verlinden, M., Bassin, S., & Zeiter, M. (2018). Legacy effects of climate extremes in alpine grassland. *Frontiers in Plant Science*, *871*. https://doi.org/10.3389/fpls.2018.01586

Defourny, P., Lamarche, C., Brockmann, C., Boettcher, M., Bontemps, S., De Maet, T., et al. (2023). Observed annual global land-use change from 1992 to 2020 three times more dynamic than reported by inventory-based statistics [Dataset]. *UCL*. Retrieved from https://maps.elie.ucl.ac.be/CCI/viewer/download.php

D'Orangeville, L., Maxwell, J., Kneeshaw, D., Pederson, N., Duchesne, L., Logan, T., et al. (2018). Drought timing and local climate determine the sensitivity of eastern temperate forests to drought. *Global Change Biology*, *24*(6), 2339–2351. https://doi.org/10.1111/gcb.14096

Dudney, J., Hallett, L. M., Larios, L., Farrer, E. C., Spotswood, E. N., Stein, C., & Suding, K. N. (2017). Lagging behind: Have we overlooked previous-year rainfall effects in annual grasslands? *Journal of Ecology*, *105*(2), 484–495. https://doi.org/10.1111/1365-2745.12671

Elliott, S., Baker, P. J., & Borchert, R. (2006). Leaf flushing during the dry season: The paradox of Asian monsoon forests. *Global Ecology and Biogeography*, *15*(3), 248–257. https://doi.org/10.1111/j.1466-822x.2006.00213.x

Foster, T. E., Schmalzer, P. A., & Fox, G. A. (2014). Timing matters: The seasonal effect of drought on tree growth. *Journal of the Torrey Botanical Society*, *141*(3), 225–241. https://doi.org/10.3159/TORREY-D-13-00060.1

Gemmer, M., Jiang, T., Su, B., & Kundzewicz, Z. W. (2008). Seasonal precipitation changes in the wet season and their influence on flood/drought hazards in the Yangtze River Basin, China. *Quaternary International*, *186*(1), 12–21. https://doi.org/10.1016/j.quaint.2007.10.001

Gupta, A., Rico-Medina, A., & Caño-Delgado, A. I. (2020). The physiology of plant responses to drought. *Science*, *368*(6488), 266–269. https://doi.org/10.1126/science.aaz7614

Hahn, C., Lüscher, A., Ernst-Hasler, S., Suter, M., & Kahmen, A. (2021). Timing of drought in the growing season and strong legacy effects determine the annual productivity of temperate grasses in a changing climate. *Biogeosciences*, *18*(2), 585–604. https://doi.org/10.5194/bg-18-585-2021

Harris, I., Osborn, T. J., Jones, P., & Lister, D. (2020). Version 4 of the CRU TS monthly high-resolution gridded multivariate climate dataset [Dataset]. *Scientific Data*, *7*(1), 109. https://doi.org/10.1038/s41597-020-0453-3

Hoek van Dijke, A. J., Orth, R., Teuling, A. J., Herold, M., Schlerf, M., Migliavacca, M., et al. (2023). Comparing forest and grassland drought responses inferred from eddy covariance and Earth observation. *Agricultural and Forest Meteorology*, *341*, 109635. https://doi.org/10.1016/j.agrformet.2023.109635

Huang, J., Yu, H., Guan, X., Wang, G., & Guo, R. (2016). Accelerated dryland expansion under climate change. *Nature Climate Change*, *6*(2), 166–171. https://doi.org/10.1038/nclimate2837

Immerzeel, W. W., Van Beek, L. P. H., & Bierkens, M. F. P. (2010). Climate change will affect the Asian water towers. *Science*, *328*(5984), 1382–1385. https://doi.org/10.1126/science.1183188

IPCC AR6 WGI. (2021). *Chapter 11: Weather and climate extreme events in a changing climate*. IPCC.

Jiang, P., Yu, Z., & Acharya, K. (2019). Drought in the western United States: Its connections with large-scale oceanic oscillations. *Atmosphere*, *10*(2), 82. https://doi.org/10.3390/ATMOS10020082

Jiao, W., Wang, L., Wang, H., Lanning, M., Chang, Q., & Novick, K. A. (2022). Comprehensive quantification of the responses of ecosystem production and respiration to drought time scale, intensity and timing in humid environments: A fluxnet synthesis. *Journal of Geophysical Research: Biogeosciences*, *127*(5). https://doi.org/10.1029/2021JG006431

Keenan, T. F., Gray, J., Friedl, M. A., Toomey, M., Bohrer, G., Hollinger, D. Y., et al. (2014). Net carbon uptake has increased through warming-induced changes in temperate forest phenology. *Nature Climate Change*, *4*(7), 598–604. https://doi.org/10.1038/nclimate2253

Kennedy, R. E., Yang, Z., Gorelick, N., Braaten, J., Cavalcante, L., Cohen, W. B., & Healey, S. (2018). Implementation of the LandTrendr algorithm on Google Earth engine [Software]. *Remote Sensing*, *10*(5), 691. https://doi.org/10.3390/rs10050691

Körner, C. (2007). The use of "altitude" in ecological research. *Trends in Ecology & Evolution*, *22*(11), 569–574. https://doi.org/10.1016/j.tree.2007.09.006

Lewis, S. L., Brando, P. M., Phillips, O. L., Van Der Heijden, G. M. F., & Nepstad, D. (2011). The 2010 Amazon drought. *Science*, *331*(6017), 554. https://doi.org/10.1126/science.1200807

Lian, X., Piao, S., Li, L. Z. X., Li, Y., Huntingford, C., Ciais, P., et al. (2020). Summer soil drying exacerbated by earlier spring greening of northern vegetation. *Science Advances*, *6*(1). https://doi.org/10.1126/sciadv.aax0255

Liu, M., Peñuelas, J., Trugman, A. T., Vargas G, G., Yang, L., & Anderegg, W. R. L. (2025). Diverging responses of terrestrial ecosystems to water stress after disturbances. *Nature Climate Change*, *15*(1), 73–79. https://doi.org/10.1038/s41558-024-02191-z

Ma, Z., Peng, C., Zhu, Q., Chen, H., Yu, G., Li, W., et al. (2012). Regional drought-induced reduction in the biomass carbon sink of Canada's boreal forests. *Proceedings of the National Academy of Sciences of the United States of America*, *109*(7), 2423–2427. https://doi.org/10.1073/pnas.1111576109

Malhi, Y., & Wright, J. (2004). Spatial patterns and recent trends in the climate of tropical rainforest regions. *Philosophical Transactions of the Royal Society B: Biological Sciences*, *359*(1443), 311–329. https://doi.org/10.1098/rstb.2003.1433

Mallick, K., Trebs, I., Boegh, E., Giustarini, L., Schlerf, M., Drewry, D. T., et al. (2016). Canopy-scale biophysical controls of transpiration and evaporation in the Amazon Basin. *Hydrology and Earth System Sciences*, *20*(10), 4237–4264. https://doi.org/10.5194/hess-20-4237-2016

McDowell, N., Pockman, W. T., Allen, C. D., Breshears, D. D., Cobb, N., Kolb, T., et al. (2008). Mechanisms of plant survival and mortality during drought: Why do some plants survive while others succumb to drought? *New Phytologist*, *178*(4), 719–739. https://doi.org/10.1111/j.1469-8137.2008.02436.x

Mckee, T. B., Doesken, N. J., & Kleist, J. (1993). The relationship of drought frequency and duration to time scales. In *Eighth Conference on Applied Climatology*.

Monteith, J. L. (1965). *Evaporation and environment*. Symposia of the Society for Experimental Biology.

Muñoz Sabater, J. (2019). ERA5-Land hourly data from 1950 to present [Dataset]. *Copernicus Climate Change Service (C3S) Climate Data Store (CDS)*. https://doi.org/10.24381/cds.e2161bac

Nemani, R. R., Keeling, C. D., Hashimoto, H., Jolly, W. M., Piper, S. C., Tucker, C. J., et al. (2003). Climate-driven increases in global terrestrial net primary production from 1982 to 1999. *Science*, *300*(5625), 1560–1563. https://doi.org/10.1126/science.1082750

Nigatu, Z. M., You, W., & Melesse, A. M. (2024). Drought dynamics in the Nile River basin: Meteorological, agricultural, and groundwater drought propagation. *Remote Sensing*, *16*(5), 919. https://doi.org/10.3390/rs16050919

Nogueira, C., Bugalho, M. N., Pereira, J. S., & Caldeira, M. C. (2017). Extended autumn drought, but not nitrogen deposition, affects the diversity and productivity of a Mediterranean grassland. *Environmental and Experimental Botany*, *138*, 99–108. https://doi.org/10.1016/j.envexpbot.2017.03.005

Peñuelas, J., Rutishauser, T., & Filella, I. (2009). Phenology feedbacks on climate change. *Science*. https://doi.org/10.1126/science.1173004

Piao, S., Liu, Q., Chen, A., Janssens, I. A., Fu, Y., Dai, J., et al. (2019). Plant phenology and global climate change: Current progresses and challenges. *Global Change Biology*, *25*(6), 1922–1940. https://doi.org/10.1111/gcb.14619

Pinzon, J. E., Pak, E. W., Tucker, C. J., Bhatt, U. S., Frost, G. V., & Macander, M. J. (2023). Global vegetation greenness (NDVI) from AVHRR GIMMS-3G+, 1981-2022 [Dataset]. *ORNL Distributed Active Archive Center*. https://doi.org/10.3334/ORNLDAAC/2187

Pompa-García, M., González-Cásares, M., Gazol, A., & Camarero, J. J. (2021). Run to the hills: Forest growth responsiveness to drought increased at higher elevation during the late 20th century. *Science of the Total Environment*, *772*, 145286. https://doi.org/10.1016/j.scitotenv.2021.145286

Prentice, I. C., Liang, X., Medlyn, B. E., & Wang, Y. P. (2015). Reliable, robust and realistic: The three R's of next-generation land-surface modelling. *Atmospheric Chemistry and Physics*, *15*(10), 5987–6005. https://doi.org/10.5194/acp-15-5987-2015

Senf, C., & Seidl, R. (2021). Persistent impacts of the 2018 drought on forest disturbance regimes in Europe. *Biogeosciences*, *18*(18), 5223–5230. https://doi.org/10.5194/bg-18-5223-2021

Silva, C. E., Kellner, J. R., Clark, D. B., & Clark, D. A. (2013). Response of an old-growth tropical rainforest to transient high temperature and drought. *Global Change Biology*, *19*(11), 3423–3434. https://doi.org/10.1111/gcb.12312

Smith, N. E., Kooijmans, L. M. J., Koren, G., Van Schaik, E., Van Der Woude, A. M., Wanders, N., et al. (2020). Spring enhancement and summer reduction in carbon uptake during the 2018 drought in northwestern Europe: Carbon uptake during 2018 Eur. drought. *Philosophical Transactions of the Royal Society B: Biological Sciences*, *375*(1810), 20190509. https://doi.org/10.1098/rstb.2019.0509

Song, L., Li, Y., Ren, Y., Wu, X., Guo, B., Tang, X., et al. (2019). Divergent vegetation responses to extreme spring and summer droughts in Southwestern China. *Agricultural and Forest Meteorology*, *279*, 107703. https://doi.org/10.1016/j.agrformet.2019.107703

Sun, S., Chen, H., Wang, G., Li, J., Mu, M., Yan, G., et al. (2016). Shift in potential evapotranspiration and its implications for dryness/wetness over Southwest China. *Journal of Geophysical Research*, *121*(16), 9342–9355. https://doi.org/10.1002/2016JD025276

Tong, X., Brandt, M., Yue, Y., Ciais, P., Rudbeck Jepsen, M., Penuelas, J., et al. (2020). Forest management in southern China generates short term extensive carbon sequestration. *Nature Communications*, *11*(1), 129. https://doi.org/10.1038/s41467-019-13798-8

Vicente-Serrano, S. M., Beguería, S., & López-Moreno, J. I. (2010). A multiscalar drought index sensitive to global warming: The standardized precipitation evapotranspiration index. *Journal of Climate*, *23*(7), 1696–1718. https://doi.org/10.1175/2009JCLI2909.1

Wang, L., Chen, W., Zhou, W., & Huang, G. (2015). Drought in Southwest China: A review. *Atmospheric and Oceanic Science Letters*, *8*(6), 339–344. https://doi.org/10.3878/AOSL20150043

Wang, S., Zhang, Y., Ju, W., Porcar-Castell, A., Ye, S., Zhang, Z., et al. (2020). Warmer spring alleviated the impacts of 2018 European summer heatwave and drought on vegetation photosynthesis. *Agricultural and Forest Meteorology*, *295*, 108195. https://doi.org/10.1016/j.agrformet.2020.108195

Wang, T., Yang, D., Zheng, G., & Shi, R. (2022). Possible negative effects of earlier thaw onset and longer thaw duration on vegetation greenness over the Tibetan Plateau. *Agricultural and Forest Meteorology*, *326*, 109192. https://doi.org/10.1016/j.agrformet.2022.109192

Wang, Y., Niu, X., Wang, B., & Song, Q. (2023). Dynamic change of forest ecological benefit of the natural forest protection project in the upper reaches of Yangtze River. *Forests*, *14*(8), 1599. https://doi.org/10.3390/f14081599

White, M. A., Thornton, P. E., & Running, S. W. (1997). A continental phenology model for monitoring vegetation responses to interannual climatic variability. *Global Biogeochemical Cycles*, *11*(2), 217–234. https://doi.org/10.1029/97GB00330

Wolf, S., Eugster, W., Ammann, C., Häni, M., Zielis, S., Hiller, R., et al. (2013). Contrasting response of grassland versus forest carbon and water fluxes to spring drought in Switzerland. *Environmental Research Letters*, *8*(3), 035007. https://doi.org/10.1088/1748-9326/8/3/035007

Wolf, S., Keenan, T. F., Fisher, J. B., Baldocchi, D. D., Desai, A. R., Richardson, A. D., et al. (2016). Warm spring reduced carbon cycle impact of the 2012 US summer drought. *Proceedings of the National Academy of Sciences of the United States of America*, *113*(21), 5880–5885. https://doi.org/10.1073/pnas.1519620113

Xiao, J. (2025). joyyyxiao/EF_paper_codes2025: Initial release (v1.0) [Software]. *Zenodo*. https://doi.org/10.5281/zenodo.14713211

Xu, B., Arain, M. A., Black, T. A., Law, B. E., Pastorello, G. Z., & Chu, H. (2020). Seasonal variability of forest sensitivity to heat and drought stresses: A synthesis based on carbon fluxes from North American forest ecosystems. *Global Change Biology*, *26*(2), 901–918. https://doi.org/10.1111/gcb.14843

Xu, L., Samanta, A., Costa, M. H., Ganguly, S., Nemani, R. R., & Myneni, R. B. (2011). Widespread decline in greenness of Amazonian vegetation due to the 2010 drought. *Geophysical Research Letters*, *38*(7). https://doi.org/10.1029/2011GL046824

Yang, K., He, J., Tang, W., Lu, H., Qin, J., Chen, Y., & Li, X. (2015). China meteorological forcing dataset (1979-2018) [Dataset]. *National Tibetan Plateau Data Center*. https://doi.org/10.11888/AtmosphericPhysics.tpe.249369.file

Yang, M., Nelson, F. E., Shiklomanov, N. I., Guo, D., & Wan, G. (2010). Permafrost degradation and its environmental effects on the Tibetan Plateau: A review of recent research. *Earth-Science Reviews*, *103*(1–2), 31–44. https://doi.org/10.1016/j.earscirev.2010.07.002

Yao, Y., Liu, Y., Song, J., Tao, S., Li, Y., Wu, T., et al. (2024). Declining tradeoff between resistance and resilience of ecosystems to drought. *Earth's Future*, *12*(5). https://doi.org/10.1029/2024EF004665

Yu, H., Luedeling, E., & Xu, J. (2010). Winter and spring warming result in delayed spring phenology on the Tibetan Plateau. *Proceedings of the National Academy of Sciences of the United States of America*, *107*(51), 22151–22156. https://doi.org/10.1073/pnas.1012490107

Zeiter, M., Schärrer, S., Zweifel, R., Newbery, D. M., & Stampfli, A. (2016). Timing of extreme drought modifies reproductive output in semi-natural grassland. *Journal of Vegetation Science*, *27*(2), 238–248. https://doi.org/10.1111/jvs.12362

Zha, T., Barr, A. G., van der Kamp, G., Black, T. A., McCaughey, J. H., & Flanagan, L. B. (2010). Interannual variation of evapotranspiration from forest and grassland ecosystems in western Canada in relation to drought. *Agricultural and Forest Meteorology*, *150*(11), 1476–1484. https://doi.org/10.1016/j.agrformet.2010.08.003

Zhang, X., Friedl, M. A., Schaaf, C. B., Strahler, A. H., Hodges, J. C. F., Gao, F., et al. (2003). Monitoring vegetation phenology using MODIS. *Remote Sensing of Environment*, *84*(3), 471–475. https://doi.org/10.1016/S0034-4257(02)00135-9

Zhou, L., Tian, Y., Myneni, R. B., Ciais, P., Saatchi, S., Liu, Y. Y., et al. (2014). Widespread decline of Congo rainforest greenness in the past decade. *Nature*, *508*(7498), 86–90. https://doi.org/10.1038/nature13265

References From the Supporting Information

Allen, R. G., Pereira, L. S., Raes, D., & Smith, M. (1998). Crop evapotranspiration—Guidelines for computing crop water requirements—FAO irrigation and drainage paper 56. *Irrigation and Drainage*. https://doi.org/10.1016/j.eja.2010.12.001

Hansen, M. C., Potapov, P. V., Moore, R., Hancher, M., Turubanova, S. A., Tyukavina, A., et al. (2013). High-resolution global maps of 21st-century forest cover change. *Science*, *342*(6160), 850–853. https://doi.org/10.1126/science.1244693

Kendall, M. G. (1975). *Rank correlation methods* (4th ed.). Charles Griffin.

Mann, H. B. (1945). Nonparametric tests against trend. *Econometrica*, *13*(3), 245. https://doi.org/10.2307/1907187

Song, X. P., Hansen, M. C., Stehman, S. V., Potapov, P. V., Tyukavina, A., Vermote, E. F., & Townshend, J. R. (2018). Global land change from 1982 to 2016. *Nature*, *560*(7720), 639–643. https://doi.org/10.1038/s41586-018-0411-9

Spearman, C. (1906). "Footrule" for measuring correlation. *British Journal of Psychology*, *2*(1), 89–108. 1904-1920. https://doi.org/10.1111/j.2044-8295.1906.tb00174.x